Computing heavy quarkonium production cross sections at high energy with the matching between collinear and high-energy factorisations

Maxim Nefedov[1]

GDR-QCD Meeting
Strqsbourg, September 28$^{\text{th.}}$, 2023

This project is supported in parts by the European Union's Horizon 2020 research and innovation programme under Grant agreement no. 824093 and the Marie Sklodowska Curie action "RadCor4HEF"

[1]Université Paris-Saclay, CNRS, IJCLab, Orsay, France

I. Quarkonium production at high energy

In collaborqtion with Jean-Philippe Lansberg and Melih Ozcelik.
Based on JHEP **05** (2022) 083; `hep-ph/2306.02425` and ongoing work

Perturbative instability of quarkonium total cross sections

Inclusive η_c-hadroproduction (CSM)

[Mangano *et.al.*, '97, ..., Lansberg, Ozcelik, '20]

$$p+p \to c\bar{c}\left[{}^1S_0^{[1]}\right]+X,\ \text{LO: } g(p_1)+g(p_2) \to c\bar{c}\left[{}^1S_0^{[1]}\right],$$

$$\sigma(\sqrt{s_{pp}}) = f_i(x_1,\mu_F) \otimes f_j(x_2,\mu_F) \otimes \hat{\sigma}(z),$$

where $z = \frac{M^2}{\hat{s}}$ with $\hat{s} = (p_1+p_2)^2$.

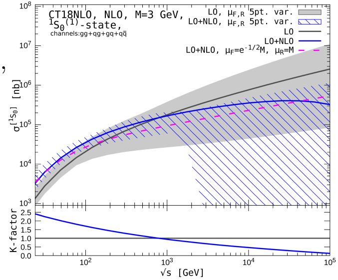

Inclusive J/ψ-photoproduction (CSM)

[Krämer, '96, ...,Colpani Serri *et.al*, '21]

$$\gamma+p \to c\bar{c}\left[{}^3S_1^{[1]}\right]+X,\ \text{LO: } \gamma(q)+g(p_1) \to c\bar{c}\left[{}^3S_1^{[1]}\right]+g,$$

$$\sigma(\sqrt{s_{\gamma p}}) = f_i(x_1,\mu_F) \otimes \hat{\sigma}(\eta),$$

where $\eta = \frac{\hat{s}-M^2}{M^2}$ with $\hat{s} = (q+p_1)^2$, $z = \frac{pP}{qP}$.

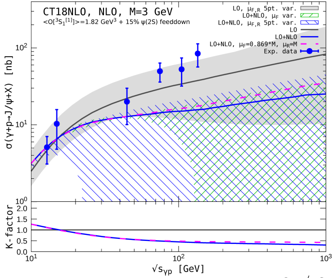

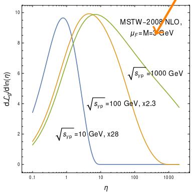

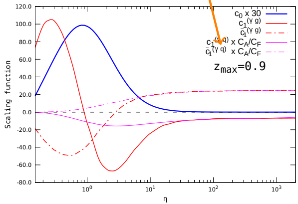

High-Energy Factorization (J/ψ photoproduction)

The **LLA** ($\sum_n \alpha_s^n \ln^{n-1}$) formalism [Collins, Ellis, '91; Catani, Ciafaloni, Hautmann, '91,'94]

Physical picture in the **LLA** for photoproduction:

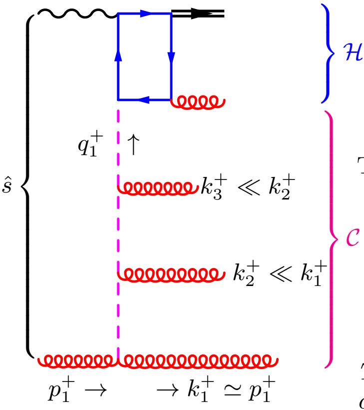

The **LLA** in $\ln \frac{1}{\xi} = \ln \frac{p_1^+}{q_1^+} \sim \ln(1+\eta)$:

$$\hat{\sigma}_{\rm HEF}^{\ln(1/\xi)}(\eta) \propto \int\limits_{1/z}^{1+\eta} \frac{dy}{y} \int\limits_0^{\infty} d\mathbf{q}_{T1}^2 \mathcal{C}\left(\frac{y}{1+\eta}, \mathbf{q}_{T1}^2, \mu_F, \mu_R\right) \mathcal{H}(y, \mathbf{q}_{T1}^2),$$

The **strict LLA** in $\ln(1+\eta) = \ln \frac{\hat{s}}{M^2}$:

$$\hat{\sigma}_{\rm HEF}^{\ln(1+\eta)}(\eta) \propto \int\limits_0^{\infty} d\mathbf{q}_{T1}^2 \mathcal{C}\left(\frac{1}{1+\eta}, \mathbf{q}_{T1}^2, \mu_F, \mu_R\right) \int\limits_{1/z}^{\infty} \frac{dy}{y} \mathcal{H}(y, \mathbf{q}_{T1}^2).$$

The LLA($\ln(1/\xi)$) contains some (N..)NLLA contributions relative to the LLA($\ln(1+\eta)$).

The coefficient function $\mathcal{H}$ has been calculated at LO [Kniehl, Vasin, Saleev, '06] and decreases as $1/y^2$ for $y \gg 1$.

High-Energy Factorization (η_c hadroproduction)

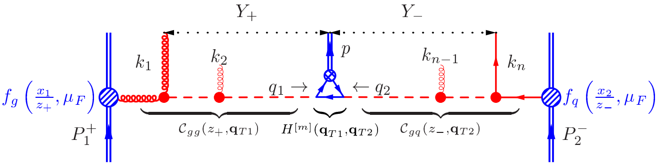

Small parameter: $z = \frac{M^2}{\hat{s}}$, LLA in $\alpha_s^n \ln^{n-1} \frac{1}{z}$:

$$\hat{\sigma}_{ij}^{[m],\ \mathrm{HEF}}(z, \mu_F, \mu_R) = \int\limits_{-\infty}^{\infty} d\eta \int\limits_{0}^{\infty} d\mathbf{q}_{T1}^2 d\mathbf{q}_{T2}^2\, \mathcal{C}_{gi}\left(\frac{M_T}{M}\sqrt{z}e^{\eta}, \mathbf{q}_{T1}^2, \mu_F, \mu_R\right)$$

$$\times \mathcal{C}_{gj}\left(\frac{M_T}{M}\sqrt{z}e^{-\eta}, \mathbf{q}_{T2}^2, \mu_F, \mu_R\right) \int\limits_{0}^{2\pi} \frac{d\phi}{2} \frac{H^{[m]}(\mathbf{q}_{T1}^2, \mathbf{q}_{T2}^2, \phi)}{M_T^4}$$

The coefficient functions $H^{[m]}$ are known at LO in α_s [Hagler *et.al*, 2000; Kniehl, Vasin, Saleev 2006] for $m = {}^1S_0^{(1,8)}, {}^3P_J^{(1,8)}, {}^3S_1^{(8)}$.
The $H^{[m]}$ is a tree-level "squared matrix element" of the $2 \rightarrow 1$-type process:

$$R_+(\mathbf{q}_{T1}, q_1^+) + R_-(\mathbf{q}_{T2}, q_2^-) \rightarrow c\bar{c}[m].$$

LLA evolution w.r.t. $\ln 1/\xi$

In the LL($\ln 1/\xi$)-approximation, the $Y = \ln 1/\xi$-evolution equation for *collinearly un-subtracted* $\tilde{\mathcal{C}}$-factor has the form:

$$\tilde{\mathcal{C}}(\xi, \mathbf{q}_T) = \delta(1-\xi)\delta(\mathbf{q}_T^2) + \hat{\alpha}_s \int\limits_{\xi}^{1} \frac{dz}{z} \int d^{2-2\epsilon}\mathbf{k}_T K(\mathbf{k}_T^2, \mathbf{q}_T^2) \tilde{\mathcal{C}}\left(\frac{\xi}{z}, \mathbf{q}_T - \mathbf{k}_T\right)$$

with $\hat{\alpha}_s = \alpha_s(\mu_R) C_A/\pi$ and

$$K(\mathbf{k}_T^2, \mathbf{q}_T^2) = \frac{1}{\pi(2\pi)^{-2\epsilon}\mathbf{k}_T^2} + \delta^{(2-2\epsilon)}(\mathbf{k}_T)\ 2\omega_g(\mathbf{q}_T^2),$$

where $\omega_g(\mathbf{q}_T^2)$ – 1-loop Regge trajectory of a gluon. It is convenient to go from $(z, \mathbf{q}_T)$-space to $(N, \mathbf{x}_T)$-space:

$$\tilde{\mathcal{C}}(N, \mathbf{x}_T) = \int d^{2-2\epsilon}\mathbf{q}_T\ e^{i\mathbf{x}_T\mathbf{q}_T} \int\limits_0^1 dx\ x^{N-1}\ \tilde{\mathcal{C}}(x, \mathbf{q}_T),$$

because:

- Mellin convolutions over z turn into products: $\int \frac{dz}{z} \to \frac{1}{N}$
- Large logs map to poles at $N=0$: $\boxed{\alpha_s^{k+1} \ln^k \frac{1}{\xi} \to \frac{\alpha_s^{k+1}}{N^{k+1}}}$
- All *collinear divergences* are contained inside $\mathcal{C}$ in $\mathbf{x}_T$-space.

Exact LL solution and the DLA

In $(N, \mathbf{q}_T)$-space, subtracted $\mathcal{C}$, which resums all terms $\propto (\hat{\alpha}_s/N)^n$ (complete LLA) has the form [Collins, Ellis, '91; Catani, Ciafaloni, Hautmann, '91,'94]:

$$\mathcal{C}(N, \mathbf{q}_T, \mu_F) = R(\gamma_{gg}(N, \alpha_s)) \frac{\gamma_{gg}(N, \alpha_s)}{\mathbf{q}_T^2} \left(\frac{\mathbf{q}_T^2}{\mu_F^2} \right)^{\gamma_{gg}(N, \alpha_s)},$$

where $\gamma_{gg}(N, \alpha_s)$ is the solution of [Jaroszewicz, '82]:

$$\frac{\hat{\alpha}_s}{N} \chi(\gamma_{gg}(N, \alpha_s)) = 1, \text{ with } \chi(\gamma) = 2\psi(1) - \psi(\gamma) - \psi(1-\gamma),$$

where $\psi(\gamma) = d \ln \Gamma(\gamma)/d\gamma$ – Euler's ψ-function. The first few terms:

$$\gamma_{gg}(N, \alpha_s) = \underbrace{\underbrace{\frac{\hat{\alpha}_s}{N}}_{\text{DLA [Blümlein, '95]}} + 2\zeta(3) \frac{\hat{\alpha}_s^4}{N^4} + 2\zeta(5) \frac{\hat{\alpha}_s^6}{N^6} + \ldots}_{\text{LLA}}$$

$\frac{\hat{\alpha}_s}{N} \leftrightarrow P_{gg}(z \to 0) = \frac{2C_A}{z} + \ldots$
The function $R(\gamma)$ is

$$R(\gamma_{gg}(N, \alpha_s)) = 1 + O(\alpha_s^3).$$

Fixed-order asymptotics from HEF

When expanded up to $O(\alpha_s)$ the HEF resummation should predict the $\hat{s} \gg M^2$ asymptotics of the CF coefficient function $\hat{\sigma}$

For the $g + g \to c\bar{c}\left[{}^1S_0^{(1)}, {}^3P_0^{(1)}, {}^3P_2^{(1)}\right]$ the NLO and NNLO($\alpha_s^2 \ln(1/z)$) terms in $\hat{\sigma}$ are predicted [M.N., Lansberg, Ozcelik '22]:

State	$A_0^{[m]}$	$A_1^{[m]}$	$A_2^{[m]}$	$B_2^{[m]}$
${}^1S_0$	1	$\mathbf{-1}$	$\frac{\pi^2}{6}$	$\frac{\pi^2}{6}$
${}^3S_1$	0	1	0	$\frac{\pi^2}{6}$
${}^3P_0$	1	$-\mathbf{\frac{43}{27}}$	$\frac{\pi^2}{6} + \frac{2}{3}$	$\frac{\pi^2}{6} + \frac{40}{27}$
${}^3P_1$	0	$\frac{5}{54}$	$-\frac{1}{9}$	$-\frac{2}{9}$
${}^3P_2$	1	$-\mathbf{\frac{53}{36}}$	$\frac{\pi^2}{6} + \frac{1}{2}$	$\frac{\pi^2}{6} + \frac{11}{9}$

$$\hat{\sigma}_{gg}^{[m]}(z \to 0) = \sigma_{\rm LO}^{[m]} \left\{ A_0^{[m]} \delta(1-z) + \frac{\alpha_s}{\pi} 2C_A \left[A_1^{[m]} + A_0^{[m]} \ln \frac{M^2}{\mu_F^2} \right] + \left(\frac{\alpha_s}{\pi}\right)^2 \ln \frac{1}{z} \cdot C_A^2 \left[2A_2^{[m]} + B_2^{[m]} + 4A_1^{[m]} \ln \frac{M^2}{\mu_F^2} + 2A_0^{[m]} \ln^2 \frac{M^2}{\mu_F^2} \right] + O(\alpha_s^3) \right\},$$

For the $\gamma + g \to c\bar{c}\left[{}^3S_1^{(1)}\right] + g$ we have computed $\eta \to \infty$ limit of the z and $\rho = \mathbf{p}_T^2/M^2$-differential NLO "scaling functions" in closed analytic form,

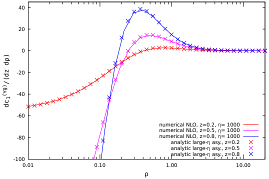

and obtained numerical results for NNLO "scaling function" c_2 in front of $\alpha_s \ln(1+\eta)$.

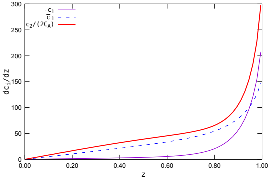

Inverse Error Weighting (InEW) matching

Development of an idea from [Echevarria *et al.*, 18'] :

$$\hat{\sigma}(\eta) = w_{\rm CF}(\eta)\hat{\sigma}_{\rm CF}(\eta) + (1 - w_{\rm CF}(\eta))\hat{\sigma}_{\rm HEF}(\eta),$$

the weights are determined through the estimates of “errors”:

$$w_{\rm CF}(\eta) = \frac{\Delta\hat{\sigma}^{-2}_{\rm CF}(\eta)}{\Delta\hat{\sigma}^{-2}_{\rm CF}(\eta) + \Delta\hat{\sigma}^{-2}_{\rm HEF}(\eta)}, \quad w_{\rm HEF}(\eta) = 1 - w_{\rm CF}(\eta).$$

- $\Delta\hat{\sigma}_{\rm CF}(\eta)$ is due to **missing higher orders and large logarithms,** it can be estimated from the α_s expansion of $\hat{\sigma}_{\rm HEF}(\eta)$.
- $\Delta\hat{\sigma}_{\rm HEF}(\eta)$ is (mostly) due to **missing power corrections in** $1/\eta$: $\Delta\hat{\sigma}_{\rm HEF}(\eta) \sim A\eta^{-\alpha_{\rm HEF}}$. We determine A and $\alpha_{\rm HEF}$ from behaviour of $\hat{\sigma}_{\rm CF}(\eta) - \hat{\sigma}_{\rm CF}(\infty)$ at $\eta \gg 1$.

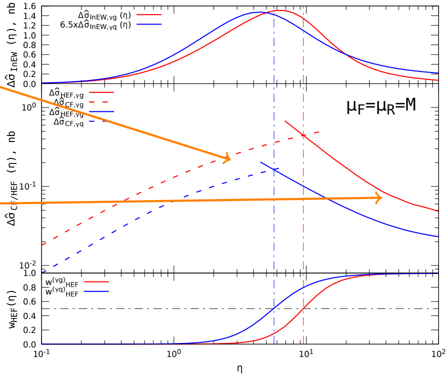

Matching with NLO

The HEF is valid in the **leading-power** in $M^2/\hat{s}$, so for $\hat{s} \sim M^2$ we match it with NLO CF by the *Inverse-Error Weighting Method* [Echevarria *et.al.*, 18'].

η_c**-hadroproduction**,
$z = M^2/\hat{s}$:

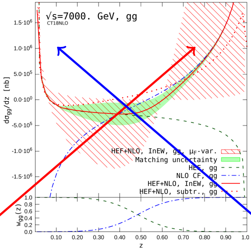

NLO **HEF**

J/ψ**-photoproduction**,
$\eta = (\hat{s} - M^2)/M^2$:

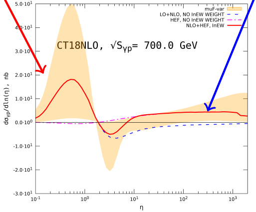

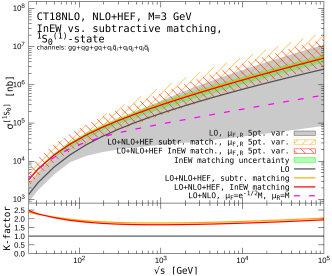

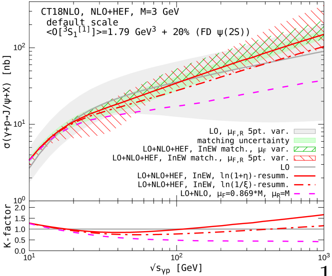

Vector quarkonium photoproduction: dynamical scale

Matched results for J/ψ photoproduction can be further improved by noticing that in the LO process:

$$\gamma(q) + g(p_1) \to Q\bar{Q}\left[{}^3S_1^{[1]}\right] + g,$$

the emitted gluon can not be soft, so that $\langle \hat{s} \rangle_{\rm LO}$ (~ 25 GeV^2 at high $\sqrt{s_{\gamma p}}$ for J/ψ) rather than M^2 can be taken as a default value of μ_F^2 and μ_R^2:

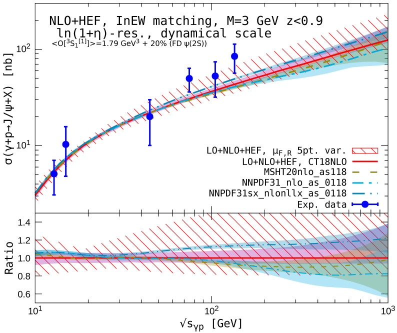

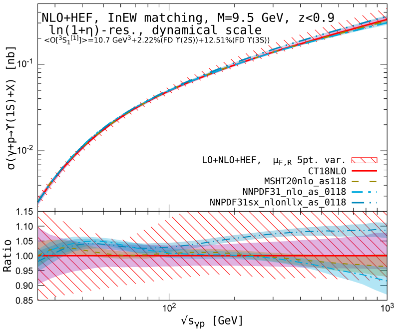

II. Beyond DLA: one-loop corrections to quarkonium impact-factors

The Gauge-Invariant EFT for Multi-Regge processes in QCD

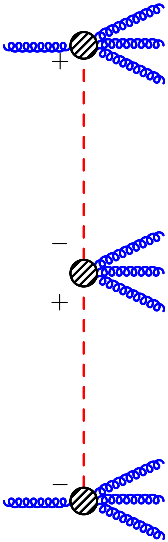

- Reggeized gluon fields $R_\pm$ carry $(k_\pm, \mathbf{k}_T, k_\mp = 0)$: $\partial_\mp R_\pm = 0$.
- **Induced interactions** of particles and Reggeons [Lipatov '95, '97; Bondarenko, Zubkov '18]:

$$L = \frac{i}{g_s} \mathrm{tr}\left[R_+ \partial_\perp^2 \partial_- \left(W[A_-] - W^\dagger[A_-]\right) + (+ \leftrightarrow -)\right],$$

with $W_{x_\mp}[x_\pm, \mathbf{x}_T, A_\pm] = P\exp\left[\frac{-ig_s}{2}\int\limits_{-\infty}^{x_\mp} dx'_\mp A_\pm(x_\pm, x'_\mp, \mathbf{x}_T)\right] = \left(1 + ig_s\partial_\pm^{-1}A_\pm\right)^{-1}$.

- Expansion of the Wilson line generates **induced vertices**:

$$\mathrm{tr}\left[R_+\partial_\perp^2 A_- + (-ig_s)(\partial_\perp^2 R_+)(A_-\partial_-^{-1}A_-) \right.$$
$$\left. + (-ig_s)^2(\partial_\perp^2 R_+)(A_-\partial_-^{-1}A_-\partial_-^{-1}A_-) + O(g_s^3) + (+\leftrightarrow -)\right].$$

- The *Eikonal propagators* $\partial_\pm^{-1} \to -i/(k^\pm)$ lead to **rapidity divergences**, which are regularized by tilting the Wilson lines from the light-cone [Hentschinski, Sabio Vera, Chachamis *et. al.*, '12-'13; M.N. '19]:

$$n_\pm^\mu \to \tilde{n}_\pm^\mu = n_\pm^\mu + r n_\mp^\mu,\ r \ll 1:\ \tilde{k}^\pm = \tilde{n}^\pm k.$$

$R\gamma \to c\bar{c}\left[{}^1S_0^{[8]}\right]$ @ 1 loop

Interference with LO:

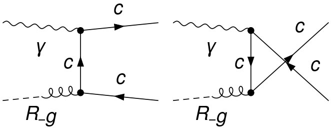

Rg-coupling diagrams:

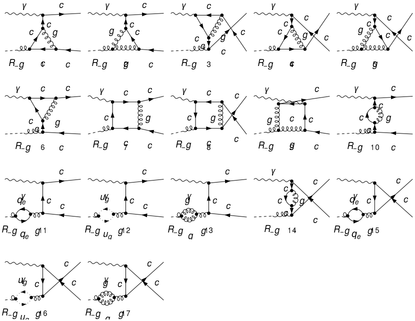

Induced *Rgg* coupling diagrams:

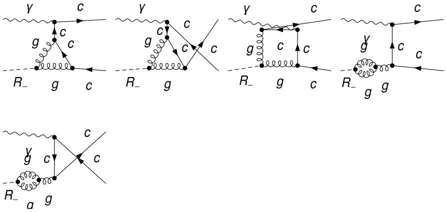

- Diagrams had been generated using custom `FeynArts` model-file, projector on the $c\bar{c}\left[{}^1S_0^{(8)}\right]$-state is inserted
- heavy-quark momenta $= p_{\mathcal{Q}}/2 \Rightarrow$ need to resolve linear dependence of quadratic denominators in some diagrams before IBP
- IBP reduction to master integrals has been performed using `FIRE`

$Rg \to c\bar{c}\left[{}^1S_0^{[1]}\right]$ and $c\bar{c}\left[{}^3S_1^{[8]}\right]$ @ 1 loop

Interference with LO: 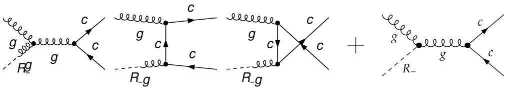

Induced Rgg coupling diagrams:

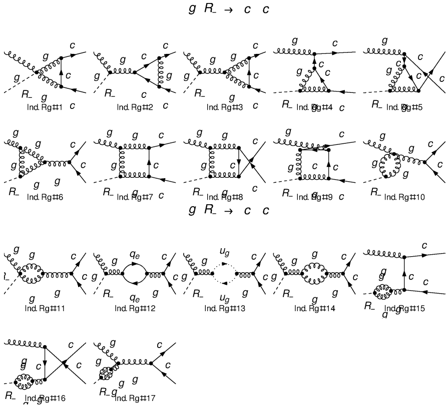

Some Rg-coupling diagrams:

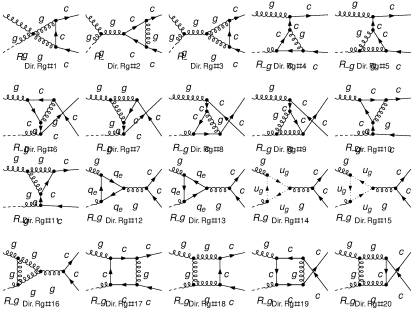

and so on...

Rapidity divergences and regularization.

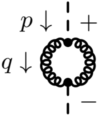

$$= g_s^2 C_A \delta_{ab} \int \frac{d^d q}{(2\pi)^D} \frac{\left(\mathbf{p}_T^2 (n_+ n_-)\right)^2}{q^2 (p-q)^2 q^+ q^-}, \quad \int \frac{dq^+ dq^-}{q^+ q^-} = \int_{y_1}^{y_2} dy \int \frac{dq^2}{q^2 + \mathbf{q}_T^2}$$

the regularization by explicit cutoff in rapidity was originally proposed [Lipatov, '95] ($q^\pm = \sqrt{q^2 + \mathbf{q}_T^2} e^{\pm y}$, $p^+ = p^- = 0$):

$$\delta_{ab} \mathbf{p}_T^2 \times \underbrace{C_A g_s^2 \int \frac{\mathbf{p}_T^2 d^{D-2} \mathbf{q}_T}{\mathbf{q}_T^2 (\mathbf{p}_T - \mathbf{q}_T)^2}}_{\omega^{(1)}(\mathbf{p}_T^2)} \times (y_2 - y_1) + \text{finite terms}$$

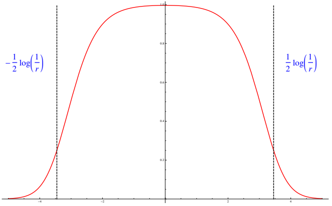

The square of regularized Lipatov vertex:

$$\Gamma_{+\mu-} \Gamma_{+\nu-} P^{\mu\nu} = \frac{16 \mathbf{q}_{T1}^2 \mathbf{q}_{T2}^2}{\mathbf{k}_T^2} f(y),$$

$$\longleftarrow f(y) = \frac{1}{(re^{-y} + e^y)^2 (re^y + e^{-y})^2},$$

$$\int_{-\infty}^{+\infty} dy \; f(y) = -1 - \log r + O(r)$$

Rapidity divergences at one loop

Only log-divergence $\sim \log r$ (Blue cells in the table) is related with Reggeization of particles in t-channel.
Integrals which **do not** have log-divergence may still contain the power-dependence on r:

- $r^{-\epsilon} \to 0$ for $r \to 0$ and $\epsilon < 0$.
- $r^{+\epsilon} \to \infty$ for $r \to 0$ and $\epsilon < 0$ – **weak-power divergence** (Pink cells in the table)
- $r^{-1+\epsilon} \to \infty$ – **power divergence.** (Red)

(# LC prop.) \ (# quadr. prop.)	1	2	3	4
1	$A_{[-]}$	$B_{[-]}$	$C_{[-]}$	…
2	$A_{[+-]}$	$B_{[+-]}$	$C_{[+-]}$	…
3	…	…	…	…

The **weak-power** and **power-divergences** cancel between Feynman diagrams describing one region in rapidity, so only log-divergences are left.

Integrals with massive internal lines

In presence of the linear denominator the massive propagator can be converted to the massless one:

$$\frac{1}{((\tilde{n}_+ l) + k_+)(l^2 - m^2)} = \frac{1}{((\tilde{n}_+ l) + k_+)(l + \kappa \tilde{n}_+)^2} + \frac{2\kappa \left[(\tilde{n}_+ l) + \frac{m^2 + \tilde{n}_+^2 \kappa^2}{2\kappa} \right]}{((\tilde{n}_+ l) + k_+)(l + \kappa \tilde{n}_+)^2 (l^2 - m^2)}$$

$\Rightarrow$ all the masses can be moved to integrals with **only quadratic propagators**. New **massless** scalar integrals with RDs arise($k^2 = 0$, $p^2 = 4m^2$, $p = q + q_1$, $q^2 = 0$):

$$\begin{aligned}
B_{[+]}(-k, k-q) &= \int \frac{d^D l}{[\tilde{l}^+](l-k)^2 (l+k-q)^2}, \\
C_{[+]}(0, -k, k-q) &= \int \frac{d^D l}{[\tilde{l}^+] l^2 (l-k)^2 (l+k-q)^2}, \\
B_{[+]}(p, k) &= \int \frac{d^D l}{[\tilde{l}^+](l+p)^2 (l+k)^2}, \\
C_{[+]}(p, k, q_1) &= \int \frac{d^D l}{[\tilde{l}^+](l+p)^2 (l+k)^2 (l+q_1)^2},
\end{aligned}$$

but they have the same complexity as already encountered ones.

Results: $R\gamma \to c\bar{c}\left[{}^1S_0^{[8]}\right]$ vs. $Rg \to c\bar{c}\left[{}^1S_0^{[1]}\right]$ @ 1 loop

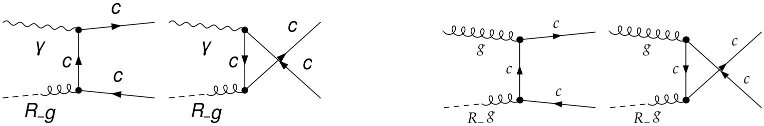

Results for $2\Re\left[\frac{H_{\text{1L x LO}}(\mathbf{q}_T)-\text{(On-shell mass CT)}}{(\alpha_s/(2\pi))H_{\text{LO}}(\mathbf{q}_T)}\right]$:

$${}^1\mathbf{S}_0^{[8]}: \left(\frac{\mu^2}{\mathbf{q}_T^2}\right)^\epsilon \frac{1}{\epsilon}\left[N_c\left(\ln\frac{\mathbf{q}_T^2}{M^2}+\ln\frac{q_-^2}{\mathbf{q}_T^2 r}+\frac{19}{6}\right)-\frac{2n_F}{3}-\frac{3}{2N_c}\right]+F_{{}^1S_0^{[8]}}(\mathbf{q}_T^2/M^2),$$

$${}^1\mathbf{S}_0^{[1]}: \left(\frac{\mu^2}{\mathbf{q}_T^2}\right)^\epsilon \left\{-\frac{N_c}{\epsilon^2}+\frac{1}{\epsilon}\left[N_c\left(\ln\frac{q_-^2}{\mathbf{q}_T^2 r}+\frac{25}{6}\right)-\frac{2n_F}{3}-\frac{3}{2N_c}\right]\right\}+F_{{}^1S_0^{[1]}}(\mathbf{q}_T^2/M^2),$$

$$F_{{}^1S_0^{[1]}}(\tau) = -\frac{10}{9}n_F+\Re[C_F F^{(C_F)}_{{}^1S_0^{[1]}}(\tau)+C_A F^{(C_A)}_{{}^1S_0^{[1]}}(\tau)],$$

$$F^{(C_F)}_{{}^1S_0^{[1]}}(\tau) = F^{(C_F)}_{{}^1S_0^{[8]}}(\tau),$$

while $F^{(C_A)}_{{}^1S_0^{[1]}}(\tau) \neq F^{(C_A)}_{{}^1S_0^{[8]}}(\tau)$.

The C_F coefficient

$$F^{(C_F)}_{{}^1S_0^{[8]}}(\tau) = \frac{\mathcal{L}_2 + \mathcal{L}_7(1-2\tau)}{\tau+1}$$
$$+\frac{1}{6(\tau+1)(2\tau+1)^2}\{144L_1\tau^2 + 144L_1\tau + 36L_1 - 16\pi^2\tau^3 - 72\tau^3 + 72\tau^3\log(2)$$
$$-156\tau^2 + 12\tau^2\log^2(2\tau+1) + 168\tau^2\log(2) - 24\left(3\tau^2+5\tau+2\right)\tau\log(\tau+1)$$
$$+12\pi^2\tau - 108\tau + 12\tau\log^2(2\tau+1) + 3\log^2(2\tau+1) + 132\tau\log(2)$$
$$+18(\tau+1)(2\tau+1)^2\log(\tau) + 4\pi^2 - 24 + 36\log(2)\}$$

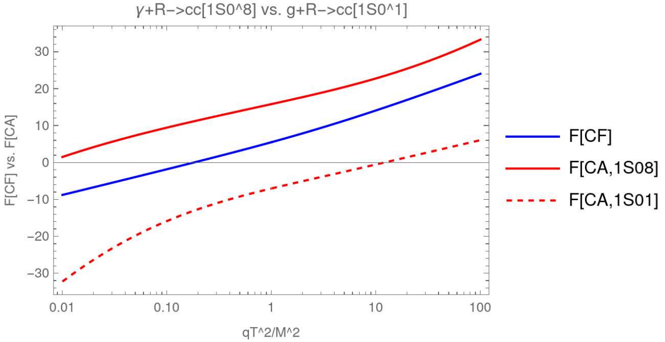

The C_A coefficient for $R\gamma \to c\bar{c}\left[{}^1S_0^{[8]}\right]$

$$
\begin{aligned}
F^{(C_A)}_{{}^1S_0^{[8]}}(\tau) \quad = \quad & \frac{1}{2(\tau-1)(\tau+1)^3}\{(\tau+1)^2\left(-4\mathcal{L}_4\left(\tau^2-1\right)+\mathcal{L}_2(\tau+1)(2\tau+1)+\mathcal{L}_7\tau(2\tau-3)+\mathcal{L}_7\right) \\
& +2\mathcal{L}_6(\tau(\tau((\tau-4)\tau-6)-4)+1)\} \\
+ \quad & \frac{1}{36(\tau-1)(\tau+1)^3(2\tau+1)}\{-216L_1\tau^4-324L_1\tau^3+108L_1\tau^2+324L_1\tau+108L_1 \\
& +120\pi^2\tau^5+608\tau^5-36\tau^5\log^2(\tau+1)+36\tau^5\log^2(2\tau+1)-36\tau^5\log^2(2) \\
& -72\tau^5\log(2)\log(\tau+1)+216\tau^5\log(\tau+1)+72\tau^5\log(2)+228\pi^2\tau^4+1520\tau^4 \\
& -306\tau^4\log^2(\tau+1)+144\tau^4\log^2(2\tau+1)-306\tau^4\log^2(2) \\
& +252\tau^4\log(2)\log(\tau+1)+432\tau^4\log(\tau+1)+360\tau^4\log(2)+84\pi^2\tau^3+608\tau^3 \\
& -360\tau^3\log^2(\tau+1)+225\tau^3\log^2(2\tau+1)-360\tau^3\log^2(2)+576\tau^3\log(2)\log(\tau+1) \\
& +72\tau^3\log(\tau+1)+72\tau^3\log(2)-120\pi^2\tau^2-1216\tau^2-108\tau^2\log^2(\tau+1) \\
& +171\tau^2\log^2(2\tau+1)-108\tau^2\log^2(2)+504\tau^2\log(2)\log(\tau+1)-360\tau^2\log(\tau+1) \\
& -360\tau^2\log(2)-72(\tau+1)^3\left(2\tau^2-\tau-1\right)\log(\tau-1)(\log(2)-\log(\tau+1)) \\
& +36(2\tau+1)\log(\tau)\left[-\tau^4+\tau^4\log(8)-6\tau^2\log(2)+\left(-\tau^3+4\tau^2+6\tau+4\right)\tau\log(\tau+1)\right. \\
& \left.-8\tau\log(2)-\log(2\tau+2)+1\right]-18\left(2\tau^5+17\tau^4+20\tau^3+6\tau^2-6\tau-3\right)\log^2(\tau) \\
& -84\pi^2\tau-1216\tau+108\tau\log^2(\tau+1)+63\tau\log^2(2\tau+1)+108\tau\log^2(2) \\
& +54\log^2(\tau+1)+9\log^2(2\tau+1)+72\tau\log(2)\log(\tau+1)-288\tau\log(\tau+1) \\
& -144\tau\log(2)-36\log(2)\log(\tau+1)-72\log(\tau+1)-12\pi^2-304+54\log^2(2)\}
\end{aligned}
$$

The C_A coefficient for $Rg \to c\bar{c}\left[{}^1S_0^{[1]}\right]$

$$
\begin{aligned}
F^{(C_A)}_{{}^1S_0^{[1]}}(\tau) \quad = \quad & \frac{1}{(\tau-1)(\tau+1)^3}\{2\mathcal{L}_1\left(\tau^2+\tau-2\right)(\tau+1)^3+\tau\left[2\mathcal{L}_5\left(\tau(\tau+1)\left(\tau^2-2\right)+1\right)\right.\\
& -\mathcal{L}_7\left(\tau^2+\tau-1\right)-\left(\mathcal{L}_2(\tau+2)(\tau+1)^2\right)+\mathcal{L}_6(\tau(\tau(6-(\tau-4)\tau)+4)-1)\Big]\\
& +2\mathcal{L}_3(\tau-1)(\tau+1)^3+2\mathcal{L}_5+\mathcal{L}_7\}\\
- \quad & \frac{1}{18(\tau-1)(\tau+1)^3}\{6\pi^2\tau^5-36\tau^5\log(2)\log(\tau+1)+36\tau^5\log(\tau+1)\log(\tau+2)+63\pi^2\tau^4\\
& -98\tau^4-63\tau^4\log^2(\tau+1)+9\tau^4\log^2(2\tau+1)-63\tau^4\log^2(2)+54\tau^4\log(2)\log(\tau+1)\\
& -36\tau^4\log(\tau+1)+36\tau^4\log(\tau+1)\log(\tau+2)+36\tau^4\log(2)+138\pi^2\tau^3-196\tau^3\\
& -72\tau^3\log^2(\tau+1)+36\tau^3\log^2(2\tau+1)-72\tau^3\log^2(2)+144\tau^3\log(2)\log(\tau+1)\\
& -36\tau^3\log(\tau+1)-72\tau^3\log(\tau+1)\log(\tau+2)-36\tau^3\log(2)+18\pi^2\tau^2\\
& -18\tau^2\log^2(\tau+1)+45\tau^2\log^2(2\tau+1)-18\tau^2\log^2(2)+108\tau^2\log(2)\log(\tau+1)\\
& +36\tau^2\log(\tau+1)-72\tau^2\log(\tau+1)\log(\tau+2)-36\tau^2\log(2)\\
& -18\left(4\tau^4+5\tau^3+\tau^2-3\tau-1\right)\log^2(\tau)+18\log(\tau)\left[\tau^5\log(2)-\tau^4(\log(4)-2)\right.\\
& \left.-\tau^3\log(4)-2\tau^2(1+\log(4))-\left(\tau^4-4\tau^3-6\tau^2-4\tau+1\right)\tau\log(\tau+1)-\tau\log(8)-\log(4)\right]\\
& -120\pi^2\tau+196\tau+36\tau\log^2(\tau+1)+18\tau\log^2(2\tau+1)+36\tau\log^2(2)+9\log^2(\tau+1)\\
& -36\tau\log(2)\log(\tau+1)+36\tau\log(\tau+1)+36\tau\log(\tau+1)\log(\tau+2)+36\tau\log(2)\\
& -36(\tau-1)(\tau+1)^3\log(\tau-1)(\log(2)-\log(\tau+1))-18\log(2)\log(\tau+1)\\
& +36\log(\tau+1)\log(\tau+2)-69\pi^2+98+9\log^2(2)\}
\end{aligned}
$$

$$
\begin{aligned}
L_1 &= \sqrt{\tau(1+\tau)}\ln\left[1+2\tau+2\sqrt{\tau(1+\tau)}\right], \\
\mathcal{L}_1 &= \mathrm{Li}_2\left(\frac{1}{\tau}+1\right) \\
\mathcal{L}_2 &= \mathrm{Li}_2\left(\frac{1}{-2\tau-1}\right) \\
\mathcal{L}_3 &= \mathrm{Li}_2\left(\frac{1}{\tau}\right)+\mathrm{Li}_2\left(\frac{\tau-1}{\tau+1}\right)-\mathrm{Li}_2\left(\frac{\tau+1}{2\tau}\right)+\frac{\mathrm{Li}_2\left(\frac{1}{4}\right)}{2}+\mathrm{Li}_2(-2) \\
\mathcal{L}_4 &= \mathrm{Li}_2\left(1+\frac{1}{\tau}\right)+\mathrm{Li}_2\left(\frac{1}{\tau}\right)+\mathrm{Li}_2\left(\frac{\tau-1}{\tau+1}\right)-\mathrm{Li}_2\left(\frac{\tau+1}{2\tau}\right)+\frac{\mathrm{Li}_2\left(\frac{1}{4}\right)}{2}+\mathrm{Li}_2(-2) \\
\mathcal{L}_5 &= \mathrm{Li}_2\left(-\frac{1}{\tau+1}\right)-\mathrm{Li}_2(\tau+2)+\frac{1}{2}\mathrm{Li}_2\left(\frac{2\tau+1}{2\tau+2}\right) \\
\mathcal{L}_6 &= -\mathrm{Li}_2\left(-\frac{2\tau+1}{\tau^2}\right)+\mathrm{Li}_2\left(-\frac{-2\tau^2+\tau+1}{2\tau^2}\right)+\mathrm{Li}_2\left(\frac{1}{2}-\frac{\tau}{2}\right)+\mathrm{Li}_2\left(-\frac{1}{\tau}\right) \\
&\quad -\mathrm{Li}_2\left(\frac{\tau-1}{2\tau}\right)-\mathrm{Li}_2(-\tau)+\mathrm{Li}_2\left(\frac{1-\tau}{\tau+1}\right) \\
\mathcal{L}_7 &= \mathrm{Li}_2(-2\tau-1)-\mathrm{Li}_2\left(\frac{2\sqrt{\tau}}{\sqrt{\tau}-\sqrt{\tau+1}}\right)-\mathrm{Li}_2\left(\frac{2\sqrt{\tau}}{\sqrt{\tau}+\sqrt{\tau+1}}\right)
\end{aligned}
$$

$R\gamma \to c\bar{c}\left[{}^1S_0^{[8]}\right]$ @ 1 loop, cross-check

In the combination of 1-loop results in the EFT:

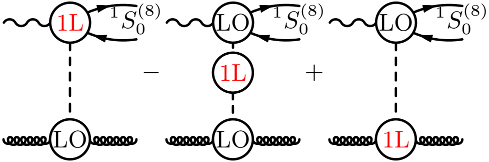

the $\ln r$ cancels and it should reproduce the the Regge limit($s \gg -t$) of the *real part* of the $2 \to 2$ 1-loop QCD amplitude:

$$\gamma + g \to c\bar{c}\left[{}^1S_0^{(8)}\right] + g.$$

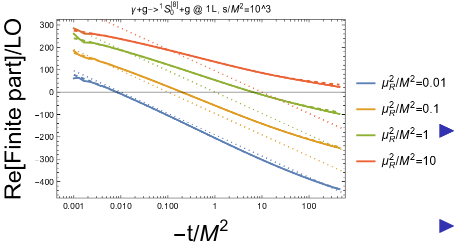

Solid lines – QCD, dashed lines – EFT, dotted lines – $-2C_A\ln(-t/\mu_R^2)\ln(s/M^2)$

- The $2 \to 2$ QCD 1-loop amplitude can be computed numerically using `FormCalc` (with some tricks, due to Coulomb divergence)
- The Regge limit of $1/\epsilon$ divergent part agrees with the EFT result
- For the finite part agreement within few % is reached, need to push to higher s

“Monster logs” in the coefficient function

In standard k_T-factorisation (or CGC/saturation) computations, where the $\sigma = \Phi(x, \mathbf{q}_T^2) \otimes \mathcal{H}(y, \mathbf{q}_T^2)$ the appearance of $\alpha_s \ln^{1,2}(\mathbf{q}_T^2/\mu^2)$ for $\mathbf{q}_T^2 \ll \mu^2$ at NLO for $\mathcal{H}$ is a serious problem. Example, Higgs-DIS in the $m_t \to \infty$ limit [M.N. ’20]:

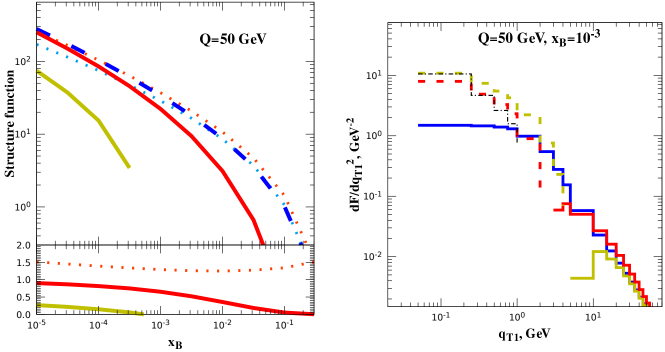

(look at yellow curves – standard MRK computation, red curves – computation with modified-MRK ≃ “kinematic constraint”)

$$\mathbf{q}_T^2 \ll Q^2 : \mathcal{H}(y, \mathbf{q}_T^2) \sim -\frac{\alpha_s C_A}{2\pi} \ln^2 \frac{\mathbf{q}_T^2}{Q^2} + \text{(single-log terms)}.$$

The "Monster logs" at small $\mathbf{q}_T$ are not scary for the matching computation

$$\hat{\sigma}_{\rm HEF}(\eta) \propto \int_0^{1+\eta} \frac{dy}{y} \int_0^{\infty} d\mathbf{q}_{T1}^2 \mathcal{C}\left(\frac{y}{1+\eta}, \mathbf{q}_{T1}^2, \mu_F, \mu_R\right) \mathcal{H}(y, \mathbf{q}_{T1}^2).$$

At NLO for $\mathcal{H}$ one typically encounters corrections $\propto \alpha_s \ln^n \frac{M^2}{\mathbf{q}_T^2}$ at $\mathbf{q}_T^2 \ll M^2$ with $n = 1, 2$. Let's study their effect in N-space (note that $\gamma_N = \hat{\alpha}_s / N$):

$$\int_0^{\mu_F^2} d\mathbf{q}_T^2 \; \mathcal{C}_{\rm DLA}(N, \mathbf{q}_T^2, \mu_F^2) \times \hat{\alpha}_s \ln^n \frac{\mu_F^2}{\mathbf{q}_T^2} = \hat{\alpha}_s \gamma_N \int_0^{\mu_F^2} \frac{d\mathbf{q}_T^2}{\mathbf{q}_T^2} \left(\frac{\mathbf{q}_T^2}{\mu_F^2}\right)^{\gamma_N} \ln^n \frac{\mu_F^2}{\mathbf{q}_T^2}$$

$$= \hat{\alpha}_s \frac{(-1)^n n!}{\gamma_N^n} = \begin{cases} -N & \text{for } n = 1 \\ \frac{2N^2}{\hat{\alpha}_s} & \text{for } n = 2 \end{cases} \xrightarrow[\text{Mellin transform}]{} \begin{cases} -\delta'(\eta) & \text{for } n = 1 \\ \frac{2}{\hat{\alpha}_s}\delta''(\eta) & \text{for } n = 2 \end{cases}$$

So these contributions *do not belong to NLA in* $\eta = (\hat{s} - M^2)/M^2 \gg 1$ and *will be removed by the matching!*

Conclusions and outlook

- The perturbative instability of p_T-integrated quarkonium production cross sections at NLO comes from the region $\hat{s} \gg M^2$
- **The problem can be solved via matching of NLO calculation at $\hat{s} \sim M^2$ and LLA HEF calculation at $\hat{s} \gg M^2$**
- The LLA HEF has to be truncated down to DLA for resummation factors, to be consistent with NLO DGLAP evolution
- The inclusive η_c hadroproduction and J/ψ photoproduction have been considered as examples
- The *next-to-DLA* calculation is needed to further reduce scale-uncertainties. Both virtual and real corrections to HEF coefficient function can be computed within the *High-Energy EFT* formalism
- **The virtual corrections to $\gamma R \to c\bar{c}[^1S0^{[8]}]$ and $gR \to c\bar{c}[^1S0^{[1]}]$ IFs had been computed**
- The logarithms $\ln M^2/\mathbf{q}_T^2$ for $\mathbf{q}_T^2 \ll M^2$ in the NLO HEF coefficient function will not be a problem for the matching calculation!

There is a lot to do even at DLA+NLO!

[Y.Feng, *et al.*, '15]

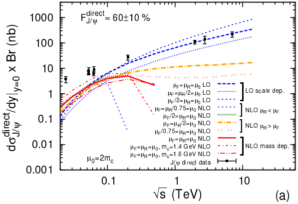

[Butenschön, He, Kniehl, '11]

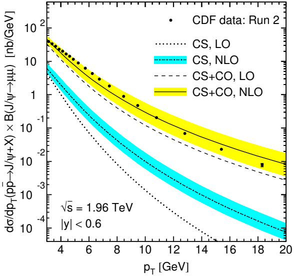

Mini workshop on overlap between QCD resummations

- 3 day mini-workshop (14–17 Jan. 2024) in "Centre Paul Langevin" in Aussois (France), right after **"Quarkonia as tools 2024"**
- Indico: `https://indico.cern.ch/event/1290502/`
- `maxim DOT nefedov AT desy DOT de`

Topics:

- Overlap between small-x and TMD resummations, rapidity divergences in both cases
- Problem of collinear/running coupling logarithms in BFKL
- BFKL beyond NLL approximation in $\mathcal{N} = 4$ SYM and QCD
- Threshold resummation
- From small to moderate x and back

Thank you for your attention!

Backup: DGLAP P_{gg} at small z

LO: $P_{gg}(z) = \frac{2C_A}{z} + \ldots \Leftrightarrow \gamma_N = \frac{\hat{\alpha}_s}{N}$

Plot from hep-ph/1607.02153 with my curve (in red) for the **strict LLA:**

$\frac{\hat{\alpha}_s}{N}\chi_{LO}(\gamma_{gg}(N)) = 1 \Rightarrow \gamma_{gg}(N) = \frac{\hat{\alpha}_s}{N} + 2\zeta(3)\frac{\hat{\alpha}_s^4}{N^4} + 2\zeta(5)\frac{\hat{\alpha}_s^6}{N^6} + \ldots$

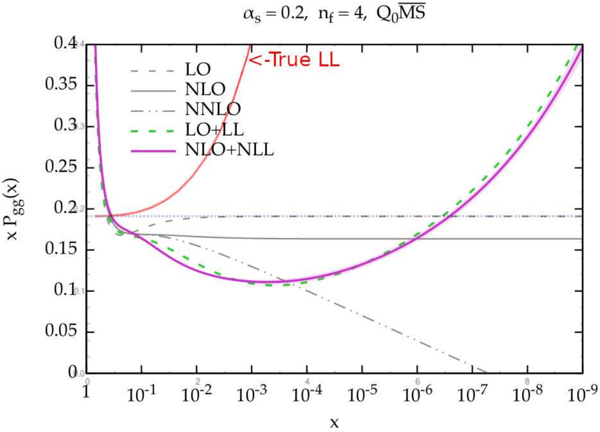

The "LO+LL" and "NLO+NLL" curves represent a form of matching between DGLAP and BFKL expansions, in a scheme by Altarelli, Ball and Forte which is more complicated than the **strict LL or NLL approximation**.

Effect of anomalous dimension beyond LO

Effect of taking **full LLA** for $\gamma_{gg}(N) = \frac{\hat{\alpha}_s}{N} + 2\zeta(3)\frac{\hat{\alpha}_s^4}{N^4} + 2\zeta(5)\frac{\hat{\alpha}_s^6}{N^6} + \ldots$ together with NLO PDF.